

Small-scale magnetic helicity losses from a mean-field dynamo

Axel Brandenburg,^{1,2*} Simon Candelaresi^{1,2} and Piyali Chatterjee³

¹*NORDITA, AlbaNova University Center, Roslagstullsbacken 23, SE 10691 Stockholm, Sweden*

²*Department of Astronomy, AlbaNova University Center, Stockholm University, SE 10691 Stockholm, Sweden*

³*Department of Astronomy and Astrophysics, Tata Institute of Fundamental Research, Colaba, Mumbai 400005, India*

Accepted 2009 June 5. Received 2009 June 5; in original form 2009 May 3

ABSTRACT

Using mean-field models with a dynamical quenching formalism, we show that in finite domains magnetic helicity fluxes associated with small-scale magnetic fields are able to alleviate catastrophic quenching. We consider fluxes that result from advection by a mean flow, the turbulent mixing down the gradient of mean small-scale magnetic helicity density or the explicit removal which may be associated with the effects of coronal mass ejections in the Sun. In the absence of shear, all the small-scale magnetic helicity fluxes are found to be equally strong for both large- and small-scale fields. In the presence of shear, there is also an additional magnetic helicity flux associated with the mean field, but this flux does not alleviate catastrophic quenching. Outside the dynamo-active region, there are neither sources nor sinks of magnetic helicity, so in a steady state this flux must be constant. It is shown that unphysical behaviour emerges if the small-scale magnetic helicity flux is forced to vanish within the computational domain.

Key words: hydrodynamics – magnetic fields – MHD – turbulence.

1 INTRODUCTION

Both mean-field theories and direct simulations of the generation of large-scale magnetic fields in astrophysical bodies, such as the Sun or the Galaxy, invoke the effects of twist. Twist is typically the result of the Coriolis force acting on ascending or descending magnetic field structures in a stratified medium. The net effect of this systematic twisting motion on the magnetic field is called the α effect. In textbooks, the α effect is normally introduced as a result of helical turbulence (Moffatt 1978; Parker 1979; Krause & Rädler 1980), but it could also arise from magnetic buoyancy instabilities (Schmitt 1987; Brandenburg & Schmitt 1998). The latter may also be at the heart of what is known as the Babcock–Leighton mechanism that describes the net effect of the tilt of decaying active regions. Mathematically, this mechanism can also be described by an α effect (Stix 1974). Regardless of all these details, any of these processes face a serious challenge connected with the conservation of magnetic helicity (Pouquet, Frisch & Léorat 1976; Kleeorin & Ruzmaikin 1982; Kleeorin, Rogachevskii & Ruzmaikin 1995). The seriousness of this is not generally appreciated, even though the conservation of magnetic helicity has long been associated with what is called catastrophic α quenching (Gruzinov & Diamond 1994, 1995, 1996). Catastrophic α quenching refers to the fact that the α effect in helical turbulence in a periodic box decreases with increasing magnetic Reynolds number for equipartition strength magnetic

fields (Vainshtein & Cattaneo 1992; Cattaneo & Hughes 1996). This would be ‘catastrophic’ because the magnetic Reynolds number is large (10^9 in the Sun and 10^{15} in the Galaxy).

A promising theory for modelling catastrophic α quenching in a mean-field simulation is the dynamical quenching approach involving an evolution equation for the α effect that follows from magnetic helicity conservation (Kleeorin & Ruzmaikin 1982). Later, Field & Blackman (2002) showed for the first time that this formalism is also able to describe the slow saturation of a helical dynamo in a triply periodic domain (Brandenburg 2001a). As this dynamo evolves towards saturation, a large-scale magnetic field builds up, but this field possesses magnetic helicity. Indeed, the eigenfunction of a homogeneous α^2 dynamo has magnetic and current helicities proportional to α . However, this concerns only the mean field, and since the helicity of the total field is conserved, the small-scale or fluctuating field must have magnetic helicity of the opposite sign (Seehafer 1996). This leads to a reduction of the α effect (Pouquet et al. 1976).

The dynamical quenching formalism is now frequently used to model the non-linear behaviour of mean-field dynamos with and without shear (Blackman & Brandenburg 2002), open or closed boundaries (Brandenburg & Subramanian 2005) and sometimes even without α effect (Yousef, Brandenburg & Rüdiger 2003; Brandenburg & Subramanian 2005). However, it soon became clear that the catastrophic quenching of the α effect can only be alleviated in the presence of magnetic helicity fluxes out of the domain (Blackman & Field 2000a,b; Kleeorin et al. 2000, 2002). There are various contributions to the magnetic helicity flux (Rogachevskii &

*E-mail: brandenb@nordita.org

Kleeorin 2000; Vishniac & Cho 2001; Subramanian & Brandenburg 2004, 2006), but one of the most obvious ones is that associated with advection. Shukurov et al. (2006) have implemented this effect in a mean-field model with dynamical quenching in order to model the effects of outflows on the evolution of the galactic magnetic field. One goal of this paper is to study this effect in more detail. In particular, it is important to clarify the consequences of boundary conditions on the local dynamics away from the boundaries. Indeed, is it really true that a helicity flux has to be maintained all the way to the boundaries, or can the helicity flux be confined to a part of the domain to alleviate catastrophic α quenching at least locally? What happens if this is not the case?

The notion of alleviating catastrophic α quenching only locally is sometimes invoked in models of the solar dynamo that rely on the production of strong magnetic fields at the bottom of the convection zone. By placing the α effect only near the surface, as is done in the interface dynamo of Parker (1993) or dynamos that are controlled by meridional circulation (Choudhuri, Schüssler & Dikpati 1995), one may evade catastrophic quenching more easily. On the other hand, as shown by Yousef et al. (2003), the effects of magnetic helicity conservation can play a role even if there is originally no α effect. It is therefore important to understand in more detail the physics of dynamical α quenching and its dependence on magnetic helicity fluxes.

Our starting point in this paper is the model of Shukurov et al. (2006), where magnetic helicity fluxes were driven by the advection from an outflow. This allows us to study the effects of varying strength of this flux in different parts of the domain. For simplicity, and in order to isolate the main effects, we ignore shear in most parts of this paper. In view of later applications to the Sun and the Galaxy, this is clearly artificial, but it helps significantly in the interpretation of the results. In particular, in the absence of shear, it is possible to have steady solutions, or at least solutions whose magnetic energy density is constant in time.

2 THE MODEL

2.1 Evolution equation of the mean field

In this paper, we consider a simple mean-field dynamo in a local one-dimensional domain. Such a model could be applicable to one hemisphere of a rotating disc or to the region close to the equator of outer stellar convection zones. Denoting the mean magnetic field by $\overline{\mathbf{B}} = \overline{\mathbf{B}}(z, t)$, the coordinate z would correspond either to the height above the mid-plane in the case of the disc or to the latitudinal distance from the equator in the case of a spherical shell. The x and y components would correspond to poloidal and toroidal fields, although in the absence of shear the two are interchangeable and cannot be distinguished. Using $\nabla \cdot \overline{\mathbf{B}} = \partial \overline{B}_z / \partial z = 0$, we have $\overline{B}_z = \text{constant} = 0$, i.e. no \overline{B}_z field is imposed. Such a mean field could be obtained by averaging the actual magnetic field over the x and y directions of a Cartesian domain.

The evolution of $\overline{\mathbf{B}}$ is governed by the Faraday equation

$$\frac{\partial \overline{\mathbf{B}}}{\partial t} = -\nabla \times \overline{\mathbf{E}}, \quad (1)$$

where $\overline{\mathbf{E}} = -(\overline{\mathbf{U}}_S + \overline{\mathbf{U}}) \times \overline{\mathbf{B}} - \overline{\mathcal{E}} + \eta \mu_0 \overline{\mathbf{J}}$ is the mean electric field, $\overline{\mathbf{U}}$ is the mean flow in the z direction, $\overline{\mathbf{U}}_S = (0, Sx, 0)$ is a linear shear flow, $\overline{\mathcal{E}}$ is the mean electromotive force, $\overline{\mathbf{J}} = \nabla \times \overline{\mathbf{B}} / \mu_0$ is the mean current density and μ_0 is the vacuum permeability. In one case, we adopt a shear parameter S that is different from zero. Since the shear is linear, we can write $\overline{\mathbf{U}}_S \times \overline{\mathbf{B}}$ as $-S \overline{A}_y \hat{\mathbf{x}}$ plus a gradient

term that can be removed by a gauge transformation. Thus, we have

$$-\overline{\mathbf{E}} = \nabla(Sx \overline{A}_y) - S \overline{A}_y \hat{\mathbf{x}} + \overline{\mathbf{U}} \times \overline{\mathbf{B}} + \overline{\mathcal{E}} - \eta \mu_0 \overline{\mathbf{J}}, \quad (2)$$

where $\overline{\mathbf{U}}$ is now the flow associated with the outflow only and does not include the shear flow. Next, we express $\overline{\mathbf{B}} = \nabla \times \overline{\mathbf{A}}$ in terms of the magnetic vector potential $\overline{\mathbf{A}}$, and solve equation (1) in its uncurled form, $\partial \overline{\mathbf{A}} / \partial t = -\overline{\mathbf{E}} - \nabla \overline{\phi}$, where $\overline{\phi}$ is the mean electrostatic potential. We perform a gauge transformation, $\overline{\mathbf{A}} \rightarrow \overline{\mathbf{A}} + \nabla \Lambda$, with the choice $\Lambda = \int (\overline{\phi} - Sx \overline{A}_y) dt$, which removes the gradient term to yield

$$\frac{\partial \overline{\mathbf{A}}}{\partial t} = -\overline{\mathbf{E}}, \quad (3)$$

which is then the final form of our equation for $\overline{\mathbf{A}}$. This form of the equation together with boundary conditions for $\overline{\mathbf{A}}$ characterizes the gauge used to calculate magnetic helicity densities and magnetic helicity fluxes for the mean field.

We solve equation (3) in the domain $0 < z < L$ and assume either a vacuum or a perfect conductor boundary condition on $z = L$. This means that on $z = L$ the mean magnetic field either vanishes, i.e. $\overline{B}_x = \overline{B}_y = 0$, or that its z derivatives vanish, i.e. $\overline{B}_{x,z} = \overline{B}_{y,z} = 0$, where a comma denotes partial differentiation. In terms of $\overline{\mathbf{A}}$, this means that on $z = L$ we have either

$$\overline{A}_{x,z} = \overline{A}_{y,z} = 0 \quad (\text{vacuum condition}), \quad (4)$$

or

$$\overline{A}_x = \overline{A}_y = 0 \quad (\text{perfect conductor condition}). \quad (5)$$

It is well known that the solutions can be in one of the two pure parity states that are either symmetric (S) or antisymmetric (A) about the mid-plane (Krause & Rädler 1980), so we have either $\overline{B}_{x,z} = \overline{B}_{y,z} = 0$ or $\overline{B}_x = \overline{B}_y = 0$ on $z = 0$. In terms of $\overline{\mathbf{A}}$,

$$\overline{A}_x = \overline{A}_y = 0 \quad \text{on } z = 0 \quad (\text{S solution}) \quad (6)$$

or

$$\overline{A}_{x,z} = \overline{A}_{y,z} = 0 \quad \text{on } z = 0 \quad (\text{A solution}). \quad (7)$$

We note that the particular boundary conditions (5) and (6) fix the value of $\overline{\mathbf{A}}$ on $z = L$ or 0, respectively. In all other combinations, the value of $\overline{\mathbf{A}}$ is not fixed and the magnetic helicity could exhibit an unphysical drift (Brandenburg, Dobler & Subramanian 2002). However, in this paper we study magnetic helicity density and its flux only in situations where either (5) or (6) is used.

We recall that, even though there is no Ω effect, i.e. no mean flow in the y direction, we shall allow for a flow $\overline{\mathbf{U}}$ in the z direction. In a disc, this would correspond to a vertical outflow, while in a star this might locally be associated with meridional circulation.

2.2 Magnetic helicity conservation

In this paper, we will study the evolution of magnetic helicity of mean and fluctuating fields. In our gauge, the evolution of the magnetic helicity density of the mean field, $h_m = \overline{\mathbf{A}} \cdot \overline{\mathbf{B}}$, is given by

$$\frac{\partial h_m}{\partial t} = 2\overline{\mathcal{E}} \cdot \overline{\mathbf{B}} - 2\eta \mu_0 \overline{\mathbf{J}} \cdot \overline{\mathbf{B}} - \nabla \cdot \overline{\mathbf{F}}_m, \quad (8)$$

where $\overline{\mathbf{F}}_m = \overline{\mathbf{E}} \times \overline{\mathbf{A}}$ is the flux of magnetic helicity of the mean magnetic field. Under the assumption of scale separation, Subramanian & Brandenburg (2006) have defined a magnetic helicity density of the small-scale field in terms of its mutual linkages.

They derived an evolution equation for the magnetic helicity density of the small-scale field,

$$\frac{\partial \bar{h}_f}{\partial t} = -2\bar{\mathcal{E}} \cdot \bar{\mathbf{B}} - 2\eta\mu_0 \bar{\mathbf{j}} \cdot \bar{\mathbf{b}} - \nabla \cdot \bar{\mathbf{F}}_f, \quad (9)$$

where $\bar{\mathbf{F}}_f$ is the flux of magnetic helicity density of the fluctuating field. Equation (9) is similar to equation (8), except that $\bar{\mathcal{E}} \cdot \bar{\mathbf{B}}$ appears with the opposite sign. This implies that turbulent amplification and diffusion of mean magnetic field (characterized by the $\bar{\mathcal{E}}$ term) cannot change the total magnetic helicity density, $\bar{h} = \bar{h}_m + \bar{h}_f$, which therefore obeys the equation

$$\frac{\partial \bar{h}}{\partial t} = -2\eta\mu_0 \bar{\mathbf{J}} \cdot \bar{\mathbf{B}} - \nabla \cdot \bar{\mathbf{F}}, \quad (10)$$

where $\bar{\mathbf{F}} = \bar{\mathbf{F}}_m + \bar{\mathbf{F}}_f$ is the total magnetic helicity flux, and $\bar{\mathbf{J}} \cdot \bar{\mathbf{B}} = \bar{\mathbf{J}} \cdot \bar{\mathbf{B}} + \bar{\mathbf{j}} \cdot \bar{\mathbf{b}}$ is the total current helicity density.

2.3 Dynamical quenching formalism

In order to satisfy the evolution equation for the total magnetic helicity density (10), we have to solve equation (9) along with equation (3), which implies that equations (8) and (10) are automatically obeyed. We assume that \bar{h}_f is proportional to $\mu_0 \bar{\mathbf{j}} \cdot \bar{\mathbf{b}}$. This $\bar{\mathbf{j}} \cdot \bar{\mathbf{b}}$ term also modifies the mean electromotive force by producing an α effect (Pouquet et al. 1976). This is sometimes referred to as the magnetic α effect,

$$\alpha_M = \frac{1}{3} \tau \bar{\mathbf{j}} \cdot \bar{\mathbf{b}} / \bar{\rho}, \quad (11)$$

where τ is the correlation time of the turbulence. In the special case of isotropy of the fluctuating field, the ratio between $\mu_0 \bar{\mathbf{j}} \cdot \bar{\mathbf{b}}$ and \bar{h}_f is k_f^2 . Direct three-dimensional turbulence simulations (details to be published elsewhere) confirm a proportionality, but the ratio between the two tends to be larger than k_f^2 . We should therefore consider k_f^2 as an adjustable parameter. In the following, we ignore compressibility effects and assume that the mean density $\bar{\rho}$ is constant.¹ Next, we assume that the turbulence is helical, so there is also a kinetic α effect proportional to the kinetic helicity,

$$\alpha_K = -\frac{1}{3} \tau \bar{\boldsymbol{\omega}} \cdot \bar{\mathbf{u}}, \quad (12)$$

where $\boldsymbol{\omega} = \nabla \times \mathbf{u}$ is the vorticity. The total α effect is then

$$\alpha = \alpha_K + \alpha_M, \quad (13)$$

and the resulting mean electromotive force is

$$\bar{\mathcal{E}} = \alpha \bar{\mathbf{B}} - \eta_t \mu_0 \bar{\mathbf{J}}, \quad (14)$$

where

$$\eta_t = \frac{1}{3} \tau \bar{u}^2 \quad (15)$$

is the turbulent magnetic diffusivity. In the following, we consider η_t and η as given and define their ratio as the magnetic Reynolds number, $R_m = \eta_t / \eta$. We shall express the strength of the magnetic field in terms of the equipartition value,

$$B_{\text{eq}} = (\mu_0 \bar{\rho} \bar{u}^2)^{1/2}, \quad (16)$$

which allows us to determine τ in the mean-field model via $\frac{1}{3} \tau = \mu_0 \bar{\rho} \eta_t / B_{\text{eq}}^2$. With these preparations, we can write the dynamical quenching formula as

$$\frac{\partial \alpha_M}{\partial t} = -2\eta_t k_f^2 \left(\frac{\bar{\mathcal{E}} \cdot \bar{\mathbf{B}}}{B_{\text{eq}}^2} + \frac{\alpha_M}{R_m} \right) - \frac{\partial}{\partial z} \bar{\mathcal{F}}_\alpha, \quad (17)$$

¹ Note that a constant mean density implies that there must exist a small-scale mass flux compensating the losses associated with the mass flux $\bar{\rho} \bar{\mathbf{U}}$.

where $\bar{\mathcal{F}}_\alpha$ is related to the mean magnetic helicity flux of the fluctuating field via

$$\bar{\mathcal{F}}_\alpha = \frac{\mu_0 \bar{\rho} \eta_t k_f^2}{B_{\text{eq}}^2} \bar{\mathbf{F}}_f. \quad (18)$$

In order to compute mean-field models, we have to solve equation (3) together with equation (17) using a closed expression for the flux $\bar{\mathcal{F}}_\alpha$. In this paper, we focus on the advective flux proportional to $\alpha_M \bar{\mathbf{U}}$, but in some cases we consider instead the effects of a turbulent magnetic helicity flux that we model by a Fickian diffusion term proportional to $-\kappa_\alpha \nabla \alpha_M$, where κ_α is a diffusion term that is either zero or otherwise a small fraction of η_t . A more natural choice might have been $\kappa_\alpha = \eta_t$, but since the effects of such diffusive magnetic helicity fluxes have never been seen in simulations, we felt that it would be more convincing if even a small fraction of η_t would lead to a notable effect.

In addition, we consider cases where we model magnetic helicity fluxes by an explicit removal of \bar{h}_f from the domain in regular time intervals Δt . Such an explicit removal of magnetic helicity associated with the fluctuating field may model the effects of coronal mass ejections, although one would expect that in reality such an approach also implies some loss of magnetic helicity associated with the large-scale field. The removal of the fluctuating magnetic field was employed by Brandenburg et al. (2002) in connection with three-dimensional turbulence simulations to demonstrate that it is, at least in principle, possible to alleviate catastrophic quenching by an artificial filtering out of small-scale turbulent magnetic fields. In this paper, we model the occasional removal of \bar{h}_f by resetting its values

$$\bar{h}_f \rightarrow \bar{h}_f - \Delta \bar{h}_f \quad \text{in regular intervals } \Delta t, \quad (19)$$

where $\Delta \bar{h}_f = \epsilon \bar{h}_f$ is chosen to be a certain fraction ϵ of the current value of \bar{h}_f . In our one-dimensional model, the corresponding expression for the flux $\Delta \bar{\mathcal{F}}_f$ can be obtained by integration, i.e.

$$\Delta \bar{\mathcal{F}}_f(z, t) = \int_0^z \Delta \bar{h}_f(z', t) dz'. \quad (20)$$

Since magnetic helicity densities and their fluxes are proportional to each other, we have simply

$$\bar{\mathcal{F}}_\alpha = \alpha_M \bar{\mathbf{U}} - \kappa_\alpha \frac{\partial \alpha_M}{\partial z} + \Delta \bar{\mathcal{F}}_\alpha, \quad (21)$$

where $\Delta \bar{\mathcal{F}}_\alpha = (\mu_0 \bar{\rho} \eta_t k_f^2 / B_{\text{eq}}^2) \Delta \bar{\mathcal{F}}_f$ is defined analogously to equation (18).

We note that the α effect will produce magnetic fields that have magnetic helicity with the same sign as that of α , and the rate of magnetic helicity production is proportional to $\alpha \bar{\mathbf{B}}^2$. In the Northern hemisphere, we have $\alpha > 0$, so the mean field should have positive magnetic helicity. We recall that shear does not contribute to magnetic helicity production, because the negative electric field associated with the shear flow, $\bar{\mathbf{U}}_S \times \bar{\mathbf{B}}$, gives no contribution to magnetic helicity production, which is proportional to $\bar{\mathcal{E}} \cdot \bar{\mathbf{B}}$, but it can still give a contribution to the flux of magnetic helicity. This is also evident if we write shear using the $-S \bar{A}_y \hat{\mathbf{x}}$ term in equation (2): after multiplying with $\bar{\mathbf{B}}$ and using $\bar{B}_x = \partial \bar{A}_y / \partial z$, we find that this term can be integrated to give just an additional flux term, $\frac{1}{2} S \bar{A}_y^2$. However, this contribution belongs clearly to the magnetic helicity flux associated with the large-scale field and is therefore unable to alleviate catastrophic quenching.

2.4 Model profiles and boundary conditions

We consider a model similar to that of Shukurov et al. (2006) who adopted linear profiles for α_K and \bar{U} of the form $\alpha_K = \alpha_0 z/H$ and $\bar{U}_z = U_0 z/H$, where the height H was chosen to be equal to the domain size, $H = L$. However, in order to separate boundary effects from effects of the dynamo we also consider the case where we extend the domain in the z direction and choose $L = 4H$ and let α_K go smoothly to zero at $z = H$ and \bar{U}_z either goes to a constant for $z > H$ or also goes smoothly to zero. Thus, we choose

$$\alpha = \alpha_0 \frac{z}{H} \Theta(z; H, w_\alpha), \quad (22)$$

where we have defined the profile function

$$\Theta(z; H, w) = \frac{1}{2} \left(1 - \tanh \frac{z-H}{w} \right), \quad (23)$$

which is unity for $z \ll H$ and zero otherwise, and w quantifies the width of this transition. For the outflow, we choose the function

$$\bar{U}_z = U_0 \frac{z}{H} [1 + (z/H)^n]^{-1/n} \Theta(z; H_U, w_U), \quad (24)$$

with $n = 20$. Both profiles are shown in Fig. 1. The strictly linear profiles of Shukurov et al. (2006) can be recovered by taking $L = H$, $w_\alpha \rightarrow 0$ and $n \rightarrow \infty$.

As length unit, we take $k_1 = \pi/2H$, and as time unit we take $(\eta_i k_1^2)^{-1}$. This deviates from Shukurov et al. (2006), who used π/H as their basic wavenumber. Our motivation for this change is that now the turbulent decay rate is equal to $\eta_i k_1^2$, without an extra 1/4 factor. We adopt non-dimensional measures for α_0 , U_0 and S , by defining

$$C_\alpha = \frac{\alpha_0}{\eta_i k_1}, \quad C_U = \frac{U_0}{\eta_i k_1} \quad \text{and} \quad C_S = \frac{S}{\eta_i k_1^2}. \quad (25)$$

To match the parameters of Shukurov et al. (2006), we note that $C_U = 0.6$ corresponds to their value of 0.3, and the value $k_f/k_1 = 10$ corresponds to their value of 5.

We obtain solutions numerically using two different codes. One code uses an explicit third-order Runge–Kutta time-stepping scheme and the other one is a semi-implicit scheme. Both schemes employ a second-order finite differences. We begin by reporting results for the original profile of Shukurov et al. (2006) with $L = H$.

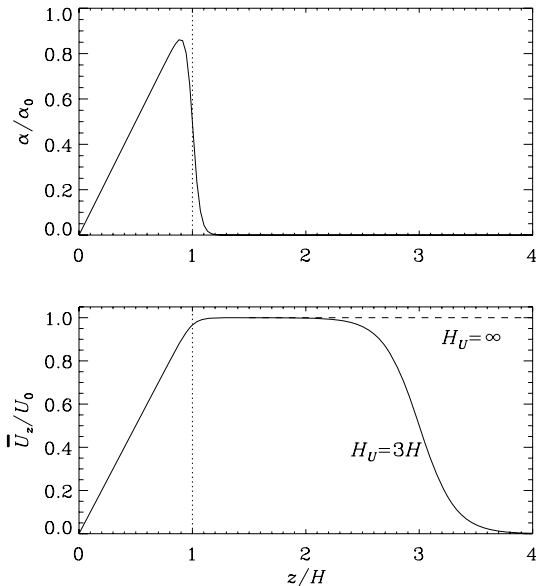


Figure 1. Profiles of α and \bar{U} for $w_\alpha k_1 = 0.2$ and $w_U k_1 = 1$.

3 RESULTS

3.1 Kinematic behaviour of the solutions

When the magnetic field is weak, the back reaction via the Lorentz force and hence the α_M term are negligible. The value of R_m then does not enter into the theory. The effects of magnetic helicity fluxes are therefore not important, so we begin by neglecting the outflow or other transporters of magnetic helicity. For the linear α profile, we find that the critical value of C_α for dynamo action to occur is about 5.13. These solutions are oscillatory with a dimensionless frequency $\bar{\omega} \equiv \omega/\eta_i k_1^2 = 1.64$. The oscillations are associated with the migration of the dynamo wave in the positive z direction. This is shown in Fig. 2 where we compare with the case of a perfectly conducting boundary condition at $z = H$ for which we find $C_\alpha^{\text{crit}} = 7.12$ and $\bar{\omega} = 2.28$.

The fact that there are oscillatory solutions to the α^2 dynamo is perhaps somewhat unusual, but it is here related to the fact that α changes sign about the equator. Similar solutions were first found by Shukurov, Sokolov & Ruzmaikin (1985) and analysed in detail by Baryshnikova & Shukurov (1987) and Rädler & Bräuer (1987). Oscillations have also been seen in other α^2 dynamos where α changes

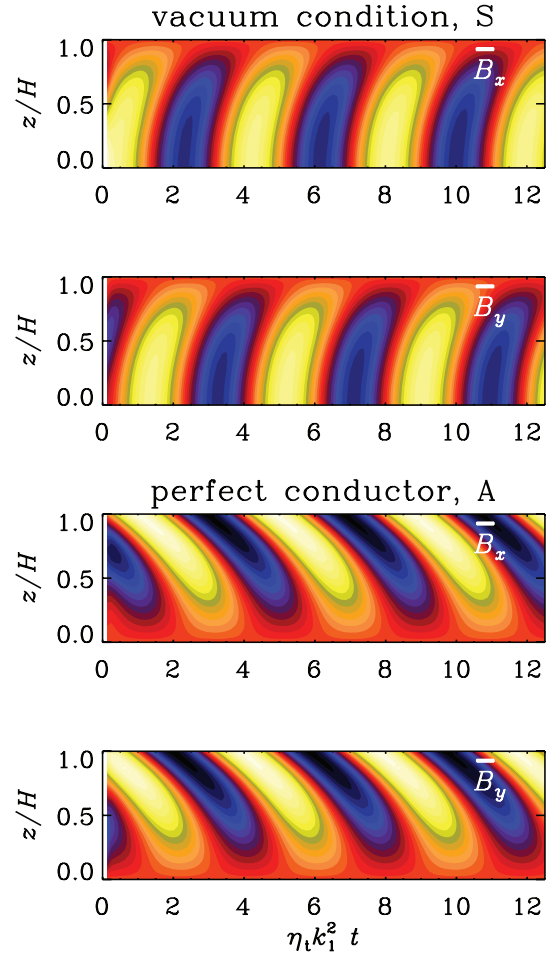


Figure 2. Space–time diagrams for \bar{B}_x and \bar{B}_y for the marginal values of C_α for $L = H$ with $C_U = 0$ and either the symmetric solution (S) with a vacuum boundary condition on $z = H$ or the antisymmetric solution (A) with the perfect conductor boundary condition. In both cases, the critical value $C_\alpha = 5.13$ is applied. Light (yellow) shades indicate positive values and dark (blue) shades indicate negative values.

sign with depth (Stefani & Gerbeth 2003; Rüdiger & Hollerbach 2004; Rüdiger, Elstner & Ossendrijver 2004; Giesecke, Ziegler & Rüdiger 2005) and in simulations of helically forced turbulence with a change of sign about the equator (Mitra et al. 2009). In the latter case, however, the outer boundaries were perfectly conducting. In our mean-field model, such a case is also oscillatory, as will be discussed below.

Note that here we have made the assumption that the solutions are symmetric about the mid-plane, i.e. $\overline{B}_i(z, t) = \overline{B}_i(-z, t)$ for $i = x$ or y . For the application to real systems, such a symmetry condition can only be justified if the symmetric solution is more easily excited than the antisymmetric one for which $\overline{B}_i(z, t) = -\overline{B}_i(-z, t)$ for $i = x$ or y . This is indeed the case when we adopt the vacuum condition at $z = H$, because the antisymmetric solution has $C_\alpha^{\text{crit}} = 7.14$ in that case. However, this is not the case for the perfect conductor boundary condition for which the antisymmetric solution has $C_\alpha^{\text{crit}} = 5.12$. We remark that there is a striking correspondence in the critical C_α values between the antisymmetric solution with perfect conductor boundary condition and the symmetric solution with vacuum condition on the one hand, and the symmetric solution with perfect conductor condition and the antisymmetric solution with vacuum condition on the other hand.

In the following, we consider both symmetric solutions using the vacuum boundary conditions, as well as antisymmetric ones using the perfect conductor boundary condition, which correspond in each case to the most easily excited mode. In the cases where we use a vacuum condition, we shall sometimes also apply an outflow. This makes the dynamo somewhat harder to excite and raises C_α^{crit} from 5.12 to 5.60 for $C_U = 0.6$, but the associated magnetic helicity flux alleviates catastrophic quenching in the non-linear case. Alternatively, we consider an explicit removal of magnetic helicity to alleviate catastrophic quenching. In cases with perfect conductor boundary conditions, the most easily excited mode is antisymmetric about the equator, which corresponds to a boundary condition that permits a magnetic helicity flux through the equator. This would not be the case for the symmetric solutions.

3.2 Saturation behaviour for different values of R_m

We now consider the saturated state for a value of C_α that is supercritical for dynamo action. In the following, we choose $C_\alpha = 8$. Throughout this paper, we assume $k_f/k_1 = 10$ for the scale separation ratio. This corresponds to the value of 5 in Shukurov et al. (2006), where k_1 was defined differently. The dynamo saturates by building up negative α_M when α_K is positive. This diminishes the total α in equation (13) and saturates the dynamo. The strength of this quenching can be alleviated by magnetic helicity fluxes that lower the negative value of α_M .

We plot in Fig. 3 the dependence of the saturation field strength $\overline{B}_{\text{sat}}$, defined here as the maximum of $|\overline{B}(z)|$ at the time of saturation. To monitor the degree of quenching, we also plot in Fig. 3 the R_m dependence of the maximum of the negative value of α_M at the time when the dynamo has saturated and reached a steady state. The maximum value of $-\alpha_M$ is lowered by about 5 per cent from 1.8 to 1.7 in units of $\eta_t k_1$ (see Fig. 3). Finally, we recall that for the α^2 dynamos considered here both \overline{B}_x and \overline{B}_y oscillate, but their relative phase shift is such that \overline{B}^2 is non-oscillatory. The normalized cycle frequency, $\tilde{\omega} \equiv \omega/\eta_t k_1$, is also plotted in Fig. 3 as a function of R_m . It is somewhat surprising that ω does not strongly depend on R_m . One may have expected that the cycle frequency could scale with the inverse resistive time $\eta_t k_1^2$. On the other hand, for oscillatory $\alpha\Omega$ dynamos the cycle frequency is known to scale with $\eta_t k_1^2$ (Blackman

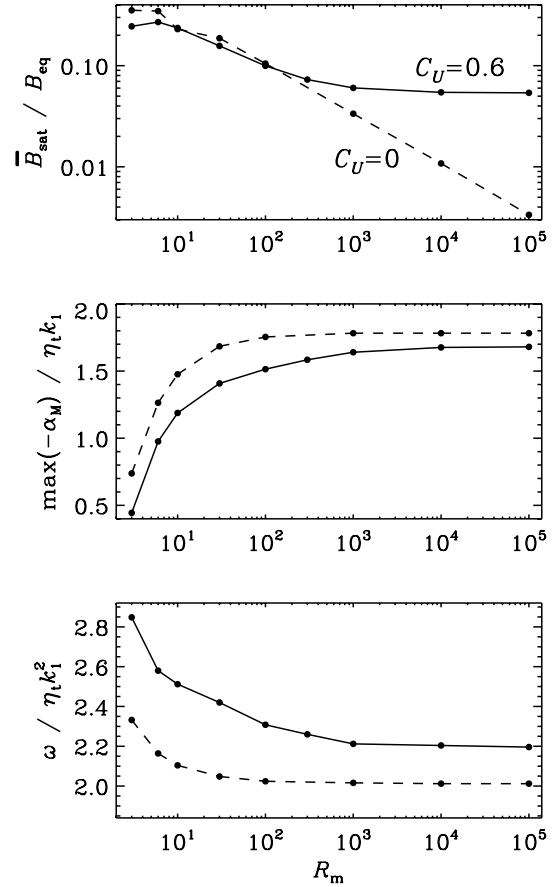


Figure 3. Scaling of the extremal value of α_M , the saturation field strength $\overline{B}_{\text{sat}}$ and the cycle frequency ω with R_m and either $C_U = 0.6$ (solid lines) or $C_U = 0$ (dashed lines).

& Brandenburg 2002), although that value could decrease if $\eta_t(\overline{B})$ is strongly quenched. However, simulations only give evidence for mild quenching (Brandenburg et al. 2008; Käpylä & Brandenburg 2009).

3.3 Helicity fluxes through the equator

We have seen in Section 3.1 that in the perfect conductor case the antisymmetric solutions are the most easily excited ones. The boundary conditions for antisymmetric solutions permit magnetic helicity transfer through the equator. A possible candidate for driving a flux through the equator would be a diffusive flux driven by the $\nabla\alpha_M$ term. In Fig. 4, we plot the R_m dependence of $\max(-\alpha_M)$, $\overline{B}_{\text{sat}}$ and $\tilde{\omega}$ for $\tilde{\kappa}_\alpha = 0.05$ and 0. Again, catastrophic α quenching is alleviated by the action of a magnetic helicity flux, but this time it is through the equator. The maximum value of $-\alpha_M$ is lowered by 15 per cent from 2.35 to 2.15 in units of $\eta_t k_1$ (see Fig. 4). Again, the cycle frequency is not changed significantly.

In Fig. 5, we compare the profiles of \overline{h}_m , \overline{h}_f , \overline{F}_m and \overline{F}_f for the most easily excited solution with vacuum and perfect conductor boundary conditions on $z = L$. In all cases, we have $\overline{h}_m = \overline{h}_f = 0$ at the mid-plane due to symmetry, and at $z = L$ we have $\overline{h}_m = 0$ and $\overline{h}_f \neq 0$. It turns out that the magnetic helicity flux of the small-scale field is balanced nearly exactly by that of the mean field. This agrees with the expectation of Blackman & Brandenburg (2003) who argued that both should be shed at nearly the same rate.

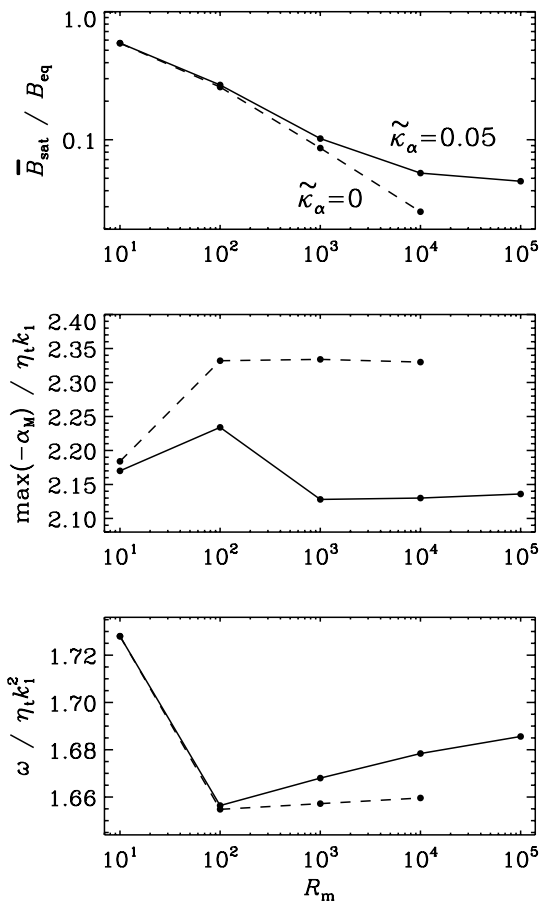


Figure 4. Same as Fig. 3, but for antisymmetric solutions in a model with perfect conductor boundary conditions with $C_U = 0$ and $\tilde{\kappa}_\alpha \equiv \kappa_\alpha/\eta_t = 0.05$ (solid lines) or 0 (dashed lines).

The ad hoc assumption of a turbulent magnetic helicity flux is plausible and has of course been made in the past (Kleeorin et al. 2002), but its effect in alleviating catastrophic quenching has not yet been seen in earlier three-dimensional turbulence simulations (Brandenburg & Dobler 2001; Brandenburg 2001b). However, except for the effects of boundaries, the conditions in those simulation were essentially homogeneous and the gradients of magnetic helicity density may have been just too small. It would therefore be important to reconsider the question of diffusive helicity fluxes in future simulations of inhomogeneous helical turbulence.

3.4 Occasional removal of \bar{h}_f

Catastrophic quenching can also be alleviated by the artificial removal of small-scale magnetic fields (see equation 19). We consider the saturation strength of the magnetic field, \bar{B}_{sat} , to characterize the alleviating effect of small-scale magnetic helicity losses. It is not surprising that the dynamo becomes stronger (\bar{B}_{sat} increases) when the fraction of small-scale field removal ϵ is increased (upper panel of Fig. 6) or the time interval of field removal is decreased (lower panel of Fig. 6). These dependencies follow approximate power laws,

$$\bar{B}_{\text{sat}}/B_{\text{eq}} \approx 0.17 \epsilon^{1/2} \approx 0.024 (\Delta t \eta_t k_1^2)^{-1/2}, \quad (26)$$

suggesting that even relatively small amounts of magnetic helicity removal in long intervals can have an effect.

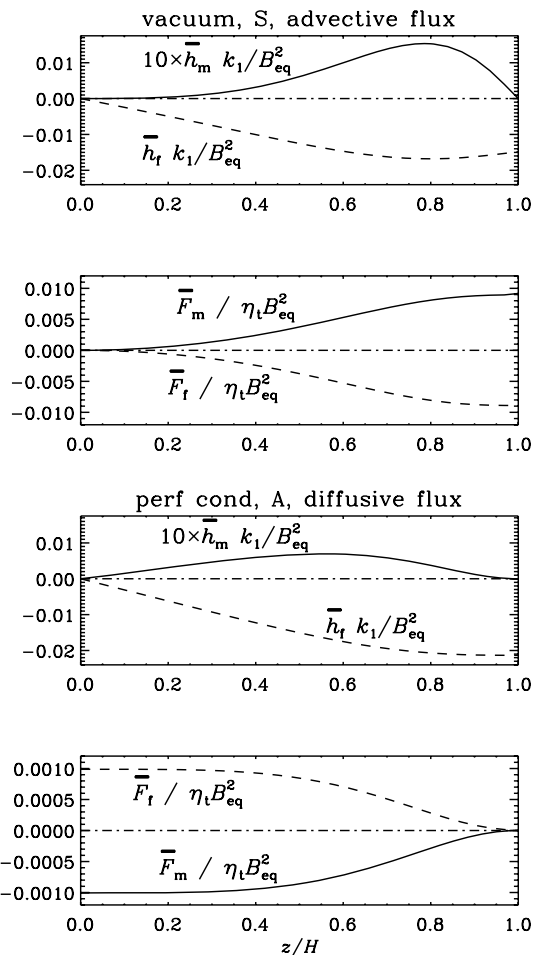


Figure 5. Mean magnetic helicity densities of mean and fluctuating fields as well as mean magnetic helicity fluxes of mean and fluctuating fields as functions of z for the S solution with vacuum boundary condition and advective flux with $C_U = 0.6$ (upper two panels) and for the A solution with perfect conductor boundary condition and diffusive flux with $\tilde{\kappa}_\alpha = 0.05$ (lower two panels). The profiles of \bar{h}_f have been scaled by a factor of 10 to make them more clearly visible. In all cases, we used $C_\alpha = 8$ and $R_m = 10^5$.

We have also performed some numerical experiments where the magnetic helicity associated with the small-scale field is only removed near the surface layers. However, in those cases the catastrophic quenching was not notably alleviated. This can be explained by noting that, in the absence of additional magnetic helicity fluxes in the interior, there is still a build-up of \bar{h}_f in the interior which quenches the α effect catastrophically.

3.5 Magnetic helicity density and flux profiles

In an attempt to understand further the evolution of magnetic helicity we have performed calculations where the magnetic helicity flux of the fluctuating field was forced to vanish at the surface. This was done by choosing a profile for \bar{U} that goes to zero at the surface. However, this invariably led to numerical problems. In order to clarify the origin of these problems we performed calculations with a taller domain, $L = 4H$, using the profiles shown in Fig. 1 and varying the value of H_U . For $H_U \rightarrow \infty$, the flux is still able to carry magnetic helicity away from the dynamo-active region into the outer layers $z > H$ (see Fig. 7). The cyclic dynamo in

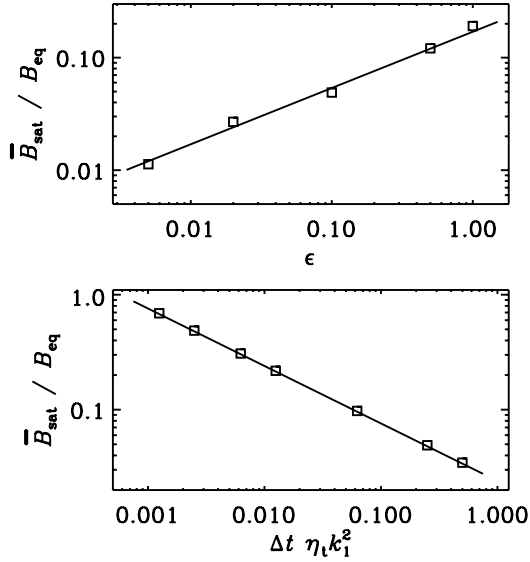


Figure 6. Saturation field strength versus ϵ for $\Delta t \eta_t k_1^2 = 0.25$ (upper panel) and versus $\Delta t \eta_t k_1^2$ for $\epsilon = 0.1$ (lower panel) in a model with $C_\alpha = 8$, $R_m = 10^5$ and $C_U = C_S = \kappa_\alpha = 0$.

$0 \leq z \leq H$ operates very much like in the case of a smaller domain (Fig. 2), except that the critical value of C_α is now lowered to $C_\alpha^{\text{crit}} = 4.32$.

However, for $H_U = 3H$ a problem arises when a parcel of positive magnetic helicity that is shed early on from the dynamo-active

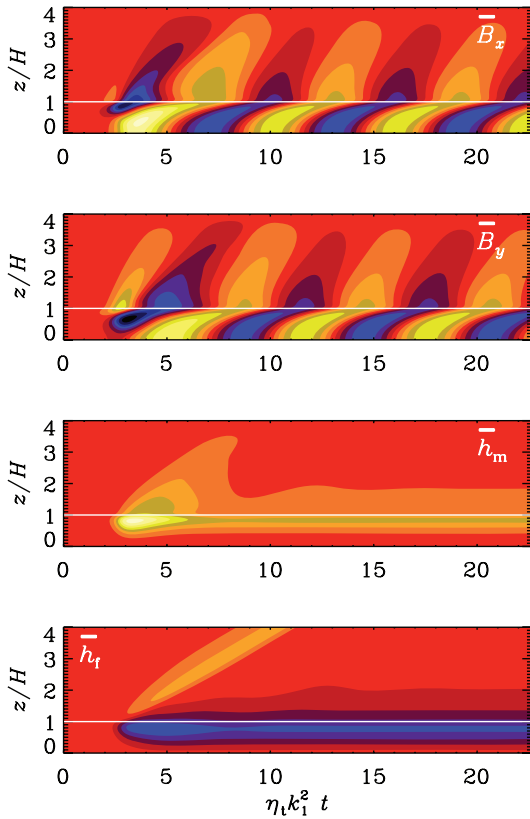


Figure 7. Space–time diagrams for \bar{B}_x and \bar{B}_y , as well as the magnetic helicity densities \bar{h}_m and \bar{h}_f for $L = 4H$, $C_\alpha = 8$, $C_U = 0.6$ and $H_U \rightarrow \infty$. The white horizontal line marks the location $z = H$. Light (yellow) shades indicate positive values and dark (blue) shades indicate negative values.

region reaches the upper layers at $z \approx 3H$, through which now no magnetic helicity can be transmitted. Positive magnetic helicity piles up into a δ function near $z \approx 3H$ until it cannot be numerically resolved any more. At higher resolution, the evolution can be followed a little longer, but the problem cannot be removed. This demonstrates again that, once a magnetic helicity flux is initiated, there is no way to stop it locally. There is also no tendency for an annihilation between magnetic helicities of mean and fluctuating fields.

The fact that positive magnetic helicity is produced is somewhat unexpected, because for $\alpha > 0$ the magnetic helicity production is positive definite. However, this can be traced back to the term $\eta_t \bar{\mathbf{J}} \cdot \bar{\mathbf{B}}$, which is part of $\bar{\mathcal{E}} \cdot \bar{\mathbf{B}}$ on the right-hand side of equation (9). Since $\bar{\mathbf{J}} \cdot \bar{\mathbf{B}}$ is positive for positive α_K , it is clear that this term produces positive \bar{h}_f just *outside* the range where α_K is finite and where it would produce \bar{h}_f of opposite sign.

In another experiment, we adopt a profile for \bar{U} such that H_U is changed from ∞ to $3H$ only after a time $t \eta_t k_1^2 = 25$, which is when the parcel of positive \bar{h}_f has left the domain. Now it is indeed negative magnetic helicity that the dynamo tries to shed and that begins to pile up near $z = 3H$. However, even though the flux is relatively weak, the blockage at $z = 3H$ leads eventually to a problem and, again, to short-wavelength oscillations indicating that the solution is numerically no longer valid.

These results suggest that the magnetic helicity flux must be allowed to continue through the rest of the domain. Of course, in reality there is the possibility of various fluxes, including diffusive fluxes that have not been included in this particular model. We note, however, that model calculations with finite κ_α in equation (21) then confirm that $\bar{F}_f(z, t)$ becomes constant in the outer parts.

3.6 Magnetic helicity with shear

It is remarkable that the magnetic helicity fluxes of the mean and fluctuating fields were always equally strong and of opposite sign. The point of this section is to underline that this is a particular property of the α^2 dynamo, and would not apply to $\alpha\Omega$ dynamos. In Fig. 8, we show the fluxes of the model with $C_\alpha = 8$ and $C_U = 0.6$, where we have varied C_S in the range from -8 to $+8$.

Shear gives rise to an additional magnetic helicity flux (Berger & Ruzmaikin 2000), and the perfect correspondence between magnetic helicity fluxes of opposite sign for mean and fluctuating fields is then broken. This additional flux of magnetic helicity is associated with the mean field and therefore does not, on its own, alleviate

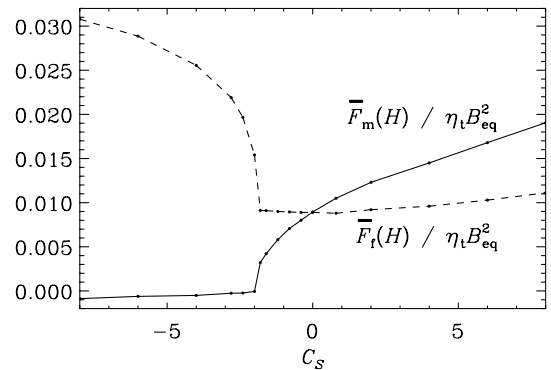


Figure 8. Dependence of $\bar{F}_m(H)$ and $\bar{F}_f(H)$ on the shear parameter for the S solution in a model with vacuum boundary condition, $C_\alpha = 8$, $C_U = 0.6$ and $R_m = 10^5$.

catastrophic quenching. However, in this model we have neglected additional magnetic helicity fluxes arising from the shear that would be associated with the fluctuating field. An example is the Vishniac–Cho flux whose effect in a mean-field model was already studied in an earlier paper (Brandenburg & Subramanian 2005). For $C < -2$, the oscillating solutions are no longer preferred and a new solution branch emerges, where the solutions are now non-oscillatory. Those are also the type of solutions studied by Shukurov et al. (2006), where $C_S = -8$ was chosen, corresponding to the value -2 in their normalization.

4 CONCLUSIONS

The present simulations have confirmed that in finite domains magnetic helicity losses through local fluxes are able to alleviate catastrophic quenching. Without such fluxes, the energy of the mean field goes to zero in the limit of large R_m , while in the presence of such fluxes $|\overline{\mathbf{B}}|$ reaches values that are about 5 per cent of the equipartition value. We emphasize at this point that this applies to the case of an α^2 dynamo. For an $\alpha\Omega$ dynamo, the mean field can reach larger values, depending on the amount of shear. For example for the model shown in Fig. 8, the field strength in units of the equipartition value rises from 5 per cent without shear to about 36 per cent with negative shear ($C_S = -8$), while for positive shear it stays around 5 per cent. We also emphasize that the difference between the two cases with and without helicity fluxes is rather weak for $R_m \leq 10^3$, so one really has to reach values around $R_m \leq 10^4$ or $R_m \leq 10^5$. Such high values of R_m are not currently feasible with three-dimensional turbulence simulations.

The other surprising result is that it is not possible to dissipate magnetic helicity flux locally once it is initiated. If the magnetic helicity flux of the small-scale field has already left the dynamo-active domain, it has to stay constant in the steady state. By adding a diffusive flux, the boundary layer in the magnetic helicity of the small-scale field could be smoothed out, but this contribution would then carry the same amount of energy as before, although now by other means.

In the presence of shear, there are additional contributions to the magnetic helicity flux associated with the mean magnetic field. There are first of all the fluxes associated with the mean field itself, but those fluxes cannot contribute to alleviating catastrophic quenching on their own. However, earlier work has shown that in the presence of shear there are also additional contributions associated with the fluctuating field (Vishniac & Cho 2001; Subramanian & Brandenburg 2004, 2006). Those terms have not been included in the present work, because they have already been studied in an earlier paper (Brandenburg & Subramanian 2005).

Several new issues have emerged from the present study. The fact that diffusive magnetic helicity fluxes through the equator can alleviate catastrophic quenching is not surprising as such, but its effects in alleviating catastrophic saturation behaviour in three-dimensional turbulence simulations have not yet been reported (Brandenburg & Dobler 2001; Brandenburg 2001b). On the other hand, simulations of forced turbulence in spherical shells with an equator did show near-equipartition strength saturation fields (Mitra et al. 2009), although the values of R_m were typically below 20, so it was not possible to draw conclusions about catastrophic quenching. A new dedicated attempt in that direction would be worthwhile using driven turbulence, but now with a linear gradient of its intensity and in the Cartesian geometry.

In view of applications to the Sun and other stars, another important development would be to extend the present work to spherical

domains. Again, some work in that direction was already reported in Brandenburg et al. (2007), but none of these models used diffusive fluxes, nor has any attempt been made to model the Sun. This would now be an important target for future research.

ACKNOWLEDGMENTS

We thank Anvar Shukurov for detailed comments and suggestions regarding an earlier version of the manuscript. We acknowledge the use of computing time at the Center for Parallel Computers at the Royal Institute of Technology in Sweden. This work was supported in part by the European Research Council under the AstroDyn Research Project 227952 and the Swedish Research Council grant 621-2007-4064.

REFERENCES

- Baryshnikova Y., Shukurov A. M., 1987, *Astron. Nachr.*, 308, 89
 Berger M. A., Ruzmaikin A., 2000, *J. Geophys. Res.*, 105, 10481
 Blackman E. G., Brandenburg A., 2002, *ApJ*, 579, 359
 Blackman E. G., Brandenburg A., 2003, *ApJ*, 584, L99
 Blackman E. G., Field G. B., 2000a, *ApJ*, 534, 984
 Blackman E. G., Field G. B., 2000b, *MNRAS*, 318, 724
 Brandenburg A., 2001a, *ApJ*, 550, 824
 Brandenburg A., 2001b, in Chossat P., Armbruster D., Iuliana O., eds, *Nato ASI Series 26, Dynamo and Dynamics, a Mathematical Challenge*. Kluwer, Dordrecht, p. 125
 Brandenburg A., Dobler W., 2001, *A&A*, 369, 329
 Brandenburg A., Schmitt D., 1998, *A&A*, 338, L55
 Brandenburg A., Subramanian K., 2005, *Astron. Nachr.*, 326, 400
 Brandenburg A., Dobler W., Subramanian K., 2002, *Astron. Nachr.*, 323, 99
 Brandenburg A., Käpylä P. J., Mitra D., Moss D., Tavakol R., 2007, *Astron. Nachr.*, 328, 1118
 Brandenburg A., Rädler K.-H., Rheinhardt M., Subramanian K., 2008, *ApJ*, 687, L49
 Cattaneo F., Hughes D. W., 1996, *Phys. Rev. E*, 54, R4532
 Choudhuri A. R., Schüssler M., Dikpati M., 1995, *A&A*, 303, L29
 Field G. B., Blackman E. G., 2002, *ApJ*, 572, 685
 Giesecke A., Ziegler U., Rüdiger G., 2005, *Phys. Earth Planet. Inter.*, 152, 90
 Gruzinov A. V., Diamond P. H., 1994, *Phys. Rev. Lett.*, 72, 1651
 Gruzinov A. V., Diamond P. H., 1995, *Phys. Plasmas*, 2, 1941
 Gruzinov A. V., Diamond P. H., 1996, *Phys. Plasmas*, 3, 1853
 Käpylä P. J., Brandenburg A., 2009, *ApJ*, 699, 1059
 Kleeorin N. I., Ruzmaikin A. A., 1982, *Magnetohydrodynamics*, 18, 116
 Kleeorin N., Rogachevskii I., Ruzmaikin A., 1995, *A&A*, 297, 159
 Kleeorin N., Moss D., Rogachevskii I., Sokoloff D., 2000, *A&A*, 361, L5
 Kleeorin N., Moss D., Rogachevskii I., Sokoloff D., 2002, *A&A*, 387, 453
 Kleeorin N., Moss D., Rogachevskii I., Sokoloff D., 2003, *A&A*, 400, 9
 Krause F., Rädler K.-H., 1980, *Mean-field Magnetohydrodynamics and Dynamo Theory*. Pergamon Press, Oxford
 Mitra M., Tavakol R., Käpylä P. J., Brandenburg A., 2009, *Phys. Rev. Lett.*, submitted
 Moffatt H. K., 1978, *Magnetic Field Generation in Electrically Conducting Fluids*. Cambridge Univ. Press, Cambridge
 Parker E. N., 1979, *Cosmical Magnetic Fields*. Clarendon Press, Oxford
 Parker E. N., 1993, *ApJ*, 408, 707
 Pouquet A., Frisch U., Léorat J., 1976, *J. Fluid Mech.*, 77, 321
 Rädler K.-H., Bräuer H.-J., 1987, *Astron. Nachr.*, 308, 101
 Rogachevskii I., Kleeorin N., 2000, *Phys. Rev. E*, 61, 5202
 Rüdiger G., Hollerbach R., 2004, *The Magnetic Universe*. Wiley-VCH, Weinheim
 Rüdiger G., Elstner D., Ossendrijver M., 2003, *A&A*, 406, 15
 Schmitt D., 1987, *A&A*, 174, 281
 Seehafer N., 1996, *Phys. Rev. E*, 53, 1283

Shukurov, A. M., Sokolov, D. D., Ruzmaikin, A. A., 1985, *Magn. Gidrodin.*, 3, 9
Shukurov A., Sokoloff D., Subramanian K., Brandenburg A., 2006, *A&A*, 448, L33
Stefani F., Gerbeth G., 2003, *Phys. Rev. E*, 67, 027302
Stix M., 1974, *A&A*, 37, 121
Subramanian K., Brandenburg A., 2004, *Phys. Rev. Lett.*, 93, 205001

Subramanian K., Brandenburg A., 2006, *ApJ*, 648, L71
Vainshtein S. I., Cattaneo F., 1992, *ApJ*, 393, 165
Vishniac E. T., Cho J., 2001, *ApJ*, 550, 752
Yousef T. A., Brandenburg A., Rüdiger G., 2003, *A&A*, 411, 321

This paper has been typeset from a \TeX/L\^AT\EX file prepared by the author.